Vandermonde-Subspace Frequency Division Multiplexing Receiver Analysis

Leonardo S. Cardoso⋆, Francisco R. P. Cavalcanti◇, Mari Kobayashi† and Mérouane Debbah⋆
⋆ Alcatel-Lucent Chair - SUPÉLEC, Gif-sur-Yvette, France
† Telecommunications Dept. - SUPÉLEC, Gif-sur-Yvette, France
◇ GTEL-DETI-UFC, Fortaleza, Brazil
{leonardo.cardoso, mari.kobayashi, merouane.debbah}@supelec.fr, rodrigo@gtel.ufc.br

***Abstract*—Vandermonde-subspace frequency division multiplexing (VFDM) is a technique for interference cancellation in overlay networks that allows a secondary network to operate simultaneously with a primary network, on the same frequency band. VFDM can be applied to block transmission systems with a guard time (or cyclic prefix) over frequency selective channels. It achieves zero interference towards the primary system by employing a special precoder that aligns the data to the null space of the interfering channel from the secondary to the primary system. In this work, we extend the assessment of VFDM by analyzing the bit error rate and sum rate capacity of practical linear receiver structures for the VFDM-based secondary system. The study realized herein serves as a basis for the implementation of a VFDM prototype system on a real transmission testbed.**

I. Introduction

In the wake of the twenty-first century, regulatory communication agencies face a new dilemma: how to increase the radio capacity using a limited radio spectrum. The fact that the allocated radio spectrum is underutilized [1] has pushed these regulatory communications agencies towards adopting a flexible spectrum management model, different from their current approach. In this model, a primary (licensed) network and a secondary (opportunistic) network are arranged in an overlay manner supporting re-utilization of resources. Cognitive radios [2] are envisioned to adopt spectrum sharing techniques [3] to offer a solution to the spectrum shortage problem.

The simplest way to perform the spectrum sharing is by exploiting the spectrum wholes of primary systems, by means of spectrum sensing techniques [4], [5]. Unfortunately, spectrum sensing has been shown to be difficult to implement due to poor reliability in the presence of fading [4], [5] and the required signaling overhead [5]. Other techniques, such as interference temperature [5], [6], dirty paper coding [7] and beamforming [5] could be used, but generally rely on unrealistic assumptions, such as prior knowledge of the messages to be transmitted or of the transceiver locations.

Recent state of the art techniques for interference alignment [8], such as the work in [9] and [10], exploit the degrees of freedom left over from the primary system to achieve the spectrum re-use. In [9], the spatial dimension is used to provide extra degrees of freedom, in contrast to the work in [10], where the frequency dimension is used instead. The main advantage of the latter work over the former relies on the fact it does not require location information or water-filling at the primary system.

The afore mentioned frequency approach, called Vandermonde-subspace frequency division multiplexing (VFDM), projects the signal to the secondary receiver on the nullspace of the channel from the secondary transmitter to the primary receiver. VFDM is a linear Vandermonde precoder that exploits the redundancy provided by the use of cyclic prefixes (or zero-paddings) of block transmission systems. VFDM benefits from the frequency selectivity of the channel to create a frequency beamformer (similar to the classical spatial beamformer). In [10], assuming perfect channel state information (CSI) at the secondary transmitter and receiver, we analyzed the achievable rates of VFDM in high SNR regime. To this end, we implicitly assumed a maximum likelihood (ML) receiver along with gaussian code books and full knowledge of the involved channels.

In this contribution, we relax the ideal assumptions made in [10] and take one step further towards the implementation of a practical VFDM system. We present and perform a numerical analysis of three classical linear equalizers in terms of bit error rate (BER) and spectral efficiency to probe the performance of VFDM, in contrast to the ML equalizer employed in our previous work. In order to assess its performance, we step away from the Gaussian code books and adopt a QPSK bit-mapping.

This work is organized as follows. In the next section, (Sec. II) we introduce the model assumed in the remainder of this work and briefly review the concept behind VFDM. We then analyze the VFDM-based receivers in Sec. III. In Sec. IV, we provide some numerical results to illustrate the analysis. Conclusions and perspectives are presented in Sec. V.

II. System Model and VFDM

We consider a cognitive interference channel, as depicted in Figure 1. This scenario is characterized by a secondary system that wishes to communicate over the same frequency band as the primary system while generating no interference. The primary system, however, has no knowledge of the existence of the secondary system (and therefore does not need to avoid interference to it).

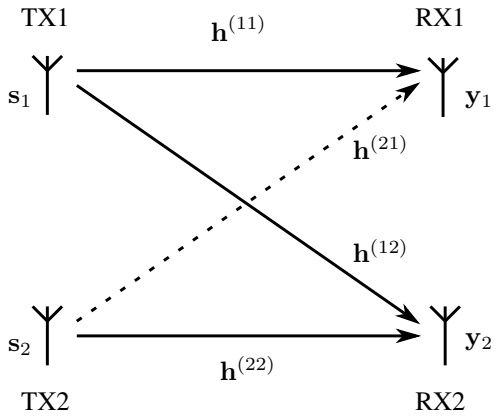

Fig. 1. Unbalanced cognitive interference channel model

In this scenario, we let $\mathbf{h}^{(ij)}$ denote the $L+1$ tap channel impulse response vector between transmitter i and receiver j. For simplicity purposes, the channels' entries are made to be unit-norm, independent and identically distributed (i.i.d.), complex circularly symmetric and Gaussian $\mathcal{CN}(0, \mathbf{I}_{L+1}/(L+1))$. The channels are i.i.d. over any pair i, j. In order to avoid block-interference, we apply orthogonal frequency division multiplexing (OFDM) with N subcarriers with a cyclic prefix of size L.

The received signals at both the primary and secondary receivers are given by:

$$\begin{aligned} \mathbf{y}_1 &= \mathbf{F}\left(\mathcal{T}(\mathbf{h}^{(11)})\mathbf{x}_1 + \mathcal{T}(\mathbf{h}^{(21)})\mathbf{x}_2 + \mathbf{n}_1\right) \\ \mathbf{y}_2 &= \mathbf{F}\left(\mathcal{T}(\mathbf{h}^{(22)})\mathbf{x}_2 + \mathcal{T}(\mathbf{h}^{(12)})\mathbf{x}_1 + \mathbf{n}_2\right), \end{aligned} \quad (1)$$

where $\mathcal{T}(\mathbf{h}^{(ij)}) \in \mathcal{C}^{N\times(N+L)}$ is a matrix with a Toeplitz structure constructed from the channel's coefficients given by

$$\mathcal{T}(\mathbf{h}^{(ij)}) = \begin{bmatrix} h_L^{(ij)} & \cdots & h_0^{(ij)} & 0 & \cdots & 0 \\ 0 & \ddots & & \ddots & \ddots & \vdots \\ \vdots & \ddots & \ddots & & \ddots & 0 \\ 0 & \cdots & 0 & h_L^{(ij)} & \cdots & h_0^{(ij)} \end{bmatrix},$$

$\mathbf{F}$ is a $N \times N$ FFT matrix with $F_{kl} = \exp(-2\pi j \frac{kl}{N})$ for $k, l = 0, \ldots, N-1$, and $\mathbf{x}_i$ denotes the transmit vector of user i of size $N+L$ subject to the individual power constraint given by

$$\text{tr}(\mathbb{E}\left[\mathbf{x}_i\mathbf{x}_i^{\text{H}}\right]) \leq (N+L)P_i, \quad (2)$$

$\mathbf{n}_i \sim \mathcal{CN}(0, \sigma\mathbf{I}_N)$ is a AWGN noise vector and the transmit power $P_i = 1$. For the primary user, we consider OFDM-modulated symbols

$$\mathbf{x}_1 = \mathbf{A}\mathbf{F}^{-1}\mathbf{s}_1 \quad (3)$$

where $\mathbf{A}$ is a $(N+L)\times N$ a cyclic prefix precoding matrix that appends the last L entries of $\mathbf{F}^{-1}\mathbf{s}_1$ and $\mathbf{s}_1$ is a symbol vector of size N with unitary norm. Regarding the secondary user, the transmit vector is given by

$$\mathbf{x}_2 = \mathbf{V}\mathbf{s}_2, \quad (4)$$

where $\mathbf{V} \in \mathcal{C}^{(N+L)\times L}$ is a linear precoder and $\mathbf{s}_2$ is the symbol vector also with unitary norm.

We have shown in [10] that, in order to cancel the interference at the primary receiver, we must to satisfy the following orthogonal condition

$$\mathcal{T}(\mathbf{h}^{(21)})\mathbf{V} = \mathbf{0}, \quad (5)$$

such that $\mathbf{V}$ belongs to the nullspace of $\mathcal{T}(\mathbf{h}^{(21)})$. Interestingly, one of the ways to define $\mathbf{V}$ by creating a Vandermonde matrix [11]

$$\mathbf{V} = \begin{bmatrix} 1 & \cdots & 1 \\ a_1 & \cdots & a_L \\ a_1^2 & \cdots & a_L^2 \\ \vdots & \ddots & \vdots \\ a_1^{N+L-1} & \cdots & a_L^{N+L-1} \end{bmatrix} \quad (6)$$

where $\{a_1, \ldots, a_L\}$ are the roots of the polynomial

$$S(z) = \sum_{i=0}^{L} h_i^{(21)} z^{L-i}$$

with $L+1$ coefficients of the channel $\mathbf{h}^{(21)}$. We have, therefore, called this technique Vandermonde-subspace Frequency Division Multiplexing (VFDM).

In this work we have chosen $\mathbf{V}$ to be the Gram-Schmidt orthonormalization of the original Vandermonde matrix structure (6) due to its better characteristics in terms of conditioning, but other methods for creating well conditioned $\mathbf{V}$ pre-coders that reside inside of the nullspace of $\mathcal{T}(\mathbf{h}^{(21)})$ and comply with (5) exist [12], [13]. Note that the construction of $\mathbf{V}$ requires full channel state information (CSI) at the secondary transmitter.

We are essentially interested in the secondary link (as the performance of the primary system is well known) and thus we concentrate on $\mathbf{y}_2$. By substituting (3) and (4) into (1) we can rewrite $\mathbf{y}_2$ as

$$\mathbf{y}_2 = \mathbf{H}_2\mathbf{s}_2 + \mathbf{H}_1\mathbf{s}_1 + \nu_2, \quad (7)$$

where $\mathbf{H}_2 = \mathbf{F}\mathcal{T}(\mathbf{h}^{(22)})\mathbf{V}$ is an $N \times L$ overall channel matrix for the secondary system, $\mathbf{H}_1 = \mathbf{F}\mathcal{T}(\mathbf{h}^{(12)})\mathbf{A}\mathbf{F}^{-1}$ is an $N \times N$ diagonal overall channel matrix for the primary system (interference w.r.t. the secondary receiver) and ν_2, the Fourier transform of the noise $\mathbf{n}_2$, has the same statistics as $\mathbf{n}_2$. We remark that VFDM converts the frequency-selective interference channel into a one-side vector Z interference channel where the primary receiver sees interference-free N parallel channels and the secondary receiver sees the interference from the primary transmitter as made clear by (7). Hence, employing an equalizer able to deal with the interference without the knowledge of the transmitted primary symbols is of interest for VFDM.

III. Equalizers Structures for VFDM

In this section we present the performance of the classical linear (MMSE, ZF and ML) equalizers for VFDM. As a starting point to construct the equalizers for VFDM let us consider the estimated symbols at the secondary receiver $\hat{\mathbf{s}}_2$ as

$$\hat{\mathbf{s}}_2 = \mathbf{G}\mathbf{y}_2. \tag{8}$$

In the following we derive the expressions for $\mathbf{G}$ for each of the studied receivers.

A. Minimum Mean Square Error

The MMSE is a well known receiver for its good performance in the presence of interference, maximizing the SINR [14]–[16]. From the MMSE definition we have that

$$\mathbf{G}_{\text{MMSE}} = \mathbf{R}_{yy}\mathbf{R}_{ys}, \tag{9}$$

where $\mathbf{R}_{yy}$ is the covariance of the received signal with itself and $\mathbf{R}_{ys}$ is the covariance of the received signal with the transmitted signal. By further developing (9) with the elements of (7) we get

$$\mathbf{G}_{\text{MMSE}} = \mathbf{H}_2^{\text{H}} \left(\mathbf{R}_{\text{I}} + \mathbf{H}_2\mathbf{H}_2^{\text{H}}\right)^{-1}, \tag{10}$$

where $\mathbf{R}_{\text{I}}$ is the covariance of the interference plus noise. By looking closely into (7) we can compute $\mathbf{R}_{\text{I}}$ as

$$\mathbf{R}_{\text{I}} = \mathbf{H}_1\mathbf{H}_1^{\text{H}} + \sigma^2\mathbf{I}_N.$$

In order to properly compute $\mathbf{G}_{\text{MMSE}}$, we are considering that the secondary receiver knows perfectly each of the overall channels $\mathbf{H}_2$ and $\mathbf{H}_1$. The channels can be obtained by pilot estimation.

We can compute the effective SINR as

$$\gamma_k = \frac{\left|\mathbf{g}_k{}^{\text{H}}\mathbf{h}_{2k}\right|^2}{\sigma^2\left|\mathbf{g}_k\mathbf{g}_k{}^{\text{H}}\right|^2 + \sum_{m=1}^{N}\left|\mathbf{g}_k{}^{\text{H}}\mathbf{h}_{1m}\right|^2 + \sum_{n=1;j\neq k}^{L}\left|\mathbf{g}_k{}^{\text{H}}\mathbf{h}_{2n}\right|^2}, \tag{11}$$

where γ_k is the individual SINR contribution for the k^{th} received symbol, $\mathbf{g}_k$ is the k^{th} column of $\mathbf{G}_{\text{MMSE}}$ and $\mathbf{h}_{ik}$ is the k^{th} column of $\mathbf{H}_i$. In the specific case for the MMSE, this expression can be further simplified to

$$\gamma_{\text{MMSE}k} = \mathbf{h}_{2k}^{\text{H}}\left(\mathbf{R}_{\text{I}} + \mathbf{U}_2\mathbf{U}_2^{\text{H}}\right)^{-1}\mathbf{h}_{2k}, \tag{12}$$

where $\mathbf{U}_2$ is an $N\times(L-1)$ matrix representing $\mathbf{H}_2$ excluding of the k^{th} column.

B. Zero Forcing

The ZF equalizer achieves a zero inter-symbol interference by assuming a peak distortion factor of zero [14]–[16]. $\mathbf{G}_{\text{ZF}}$ is the ZF equalization filter given by

$$\mathbf{G}_{\text{ZF}} = {\mathbf{H}_2}^{-1}.$$

In the case of the rectangular overall channel matrix $\mathbf{H}_2$, the inversion is accomplished by the pseudo-inverse operation (defined by $\mathbf{A}^\star = (\mathbf{A}_2^{\text{H}}\mathbf{A}_2)^{-1}\mathbf{A}_2^{\text{H}}$), and thus

$$\mathbf{G}_{\text{ZF}} = {\mathbf{H}_2}^\star. \tag{13}$$

Here we consider that the secondary receiver possesses only an estimate for the overall channel $\mathbf{H}_2$, obtained as described in the MMSE case. The ZF does not take into account the outside interference as for the case of the MMSE, and is thus simpler. Similar to the MMSE case, the ZF equalizer's SINR is given by taking $\mathbf{g}_k$ as the k^{th} column of $\mathbf{G}_{\text{ZF}}$ in (11).

C. Matched Filter

Unlike the previous two equalizers, the MF correlates the received symbols with a filter that matches the channel, hence its name [14]–[16]. This is accomplished by convolving the received signal with a time reversed version of the overall channel matrix, and therefore, $\mathbf{G}_{\text{MF}}$ is the MF equalization filter given by

$$\mathbf{G}_{\text{MF}} = \mathbf{H}_2^{\text{H}}. \tag{14}$$

The SINR can be expressed similarly to the MMSE and ZF cases, by taking $\mathbf{g}_k$ as the k^{th} column of $\mathbf{G}_{\text{MF}}$ in (11).

For all the SINR expressions given above, all symbols have the same statistical behavior, and thus, we can consider that the average bit error probability [17] for QPSK to be given by

$$P_{\text{e}} = \frac{1}{L}\sum_{k=1}^{L}\mathbb{E}\left[Q\left(\sqrt{\gamma_k}\right)\right],$$

where $Q(\cdot)$ is the Q-function.

IV. Numerical Analysis

In this section we provide some numerical results to illustrate the performance of the equalizers for VFDM. The results presented were inspired by the 802.11a standard [18], in the sense that we adopt $N = 64$, $L = 16$ and OFDM symbol time t_{blk} of 4 μs (3.2 μs of useful data and 0.8 μs of guard interval). The adopted bit-mapping is the quadrature phase shift keying (QPSK) for both the primary and secondary transmissions. Channels and noise are generated according to the definitions made in section II. Monte Carlo based simulations are executed until the target BER is reached with a statistically relevant amount of samples. Again, we assume perfect knowledge of all channels involved. The simulated BER is computed as the ratio between the number of erroneous bits and the total number of transmitted bits per block, which is further averaged over the total amount of blocks. In order to show a different point of view of the receiver performance,

we also include throughput results, which are calculated as $T = (1 - \text{BER}) \cdot n_{\text{bits}}/t_{\text{blk}}$, where n_{bits} is the number of bits per block. For the following results, we have added a cross interference factor $\alpha \in [0, 1]$ to scale the interference coming from the primary system, such that (7) becomes

$$\mathbf{y}_2 = \mathbf{H}_2\mathbf{s}_2 + \alpha\mathbf{H}_1\mathbf{s}_1 + \nu_2.$$

A. VFDM with respect to OFDM

We start by focusing on the secondary system, comparing its BER with a known reference point, in our case the primary OFDM system. For such, we have chosen the MMSE equalizer for both (although results are extendable to the other receivers), and set $\alpha = 0$ in order to cancel all interference coming from the primary system to rule out its effect on the assessment. For the OFDM case, the BER, P_e and T are calculated the same way as for the VFDM case. We have adapted equations (10) and (11) to OFDM's own overall channel (substituting $\mathbf{H}_2$ for $\mathbf{F}\mathcal{T}(\mathbf{h}^{(11)})\mathbf{A}\mathbf{F}^{-1}$) and taking the inverse instead of the pseudo-inverse.

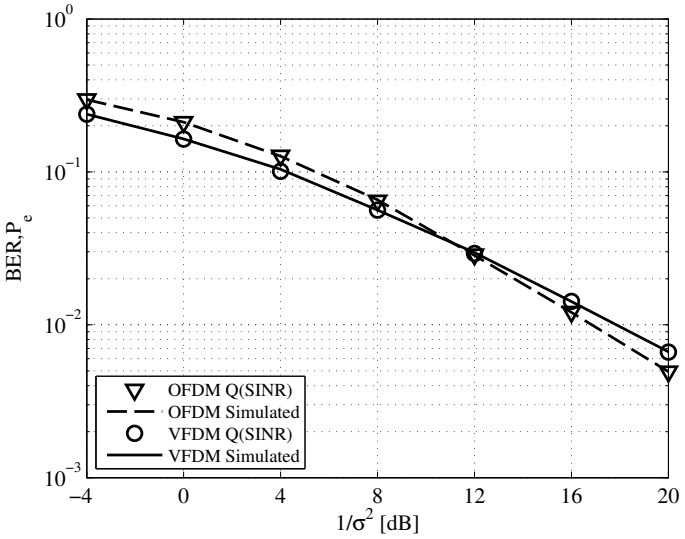

Fig. 2. Comparative MMSE equalizer BER and P_e for the primary (OFDM) and secondary (VFDM) systems ($N = 64$, $L = 16$, $\alpha = 0$).

Figure 2 presents the BER performances of VFDM and OFDM versus SNR ($1/\sigma^2$). Even though VFDM and OFDM are both based on orthogonal frequency modulators, since VFDM transmits L symbols over N dimensions it experiences a diversity gain in comparison to OFDM, which transmits the same amount of symbols as available dimensions. Therefore, by coding L symbols over N useful carriers VFDM effectively provides a symbol redundancy with respect to the noise realization. This noise robustness explains the better BER performance of VFDM at low SNR regime (Figure 2), where it experiences a higher symbol to noise robustness. Bear in mind that even though VFDM provides a gain in terms of BER, it still is limited in terms of throughput, as seen on Figure 3, since its rate is bounded to L/N times the throughput of OFDM as shown previously in [10]. It is also important to note that since the transmitted signal for OFDM and VFDM has a constant unitary energy per block, then VFDM's transmitted energy per symbol has to be scaled up by a factor of N/L, compared to the OFDM's one.

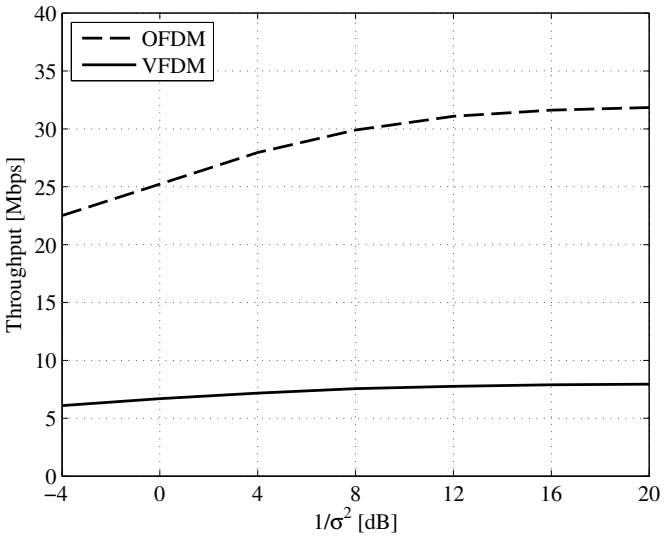

Fig. 3. Comparative MMSE equalizer throughput T for the primary (OFDM) and secondary (VFDM) systems ($N = 64$, $L = 16$, $\alpha = 0$).

B. Equalizers for VFDM

Although it is already expected that the MMSE equalizer provides the best performance for VFDM among the studied equalizers, due to its inherent capability to deal with interference, it is interesting to see how the other equalizers behave in terms of BER and throughput. Again, in order to properly assess the performance contribution of each equalizer structure by themselves, we have chosen to disable the interference from the primary system ($\alpha = 0$). In Figure 4 the BER and P_e performances are presented for the three equalizers focus of this work. As expected the MMSE outperforms the two other

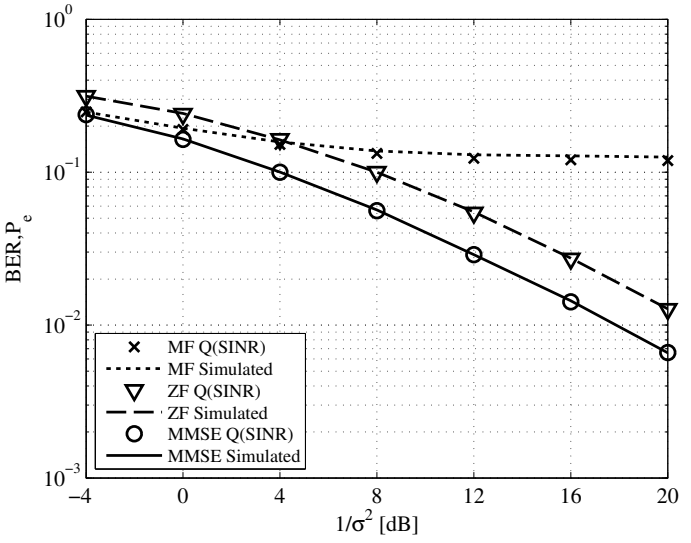

Fig. 4. Comparative BER and P_e for the MMSE, ZF and MF equalizers for the secondary (VFDM) system ($N = 64$, $L = 16$, $\alpha = 0$).

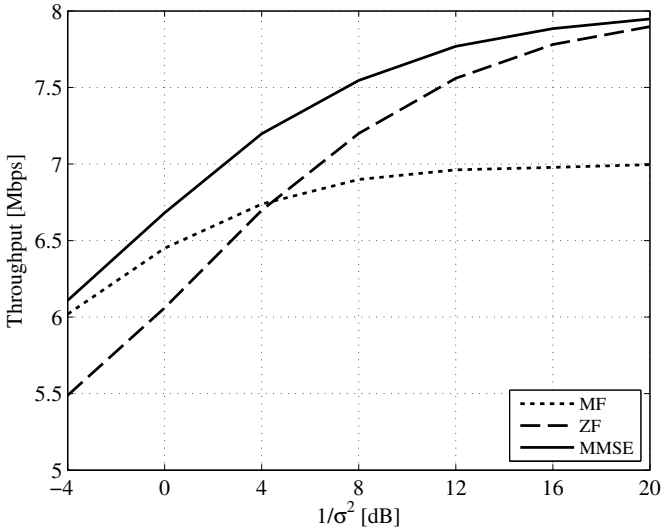

Fig. 5. Comparative throughput T for the MMSE, ZF and MF equalizers for the secondary (VFDM) system ($N = 64$, $L = 16$, $\alpha = 0$).

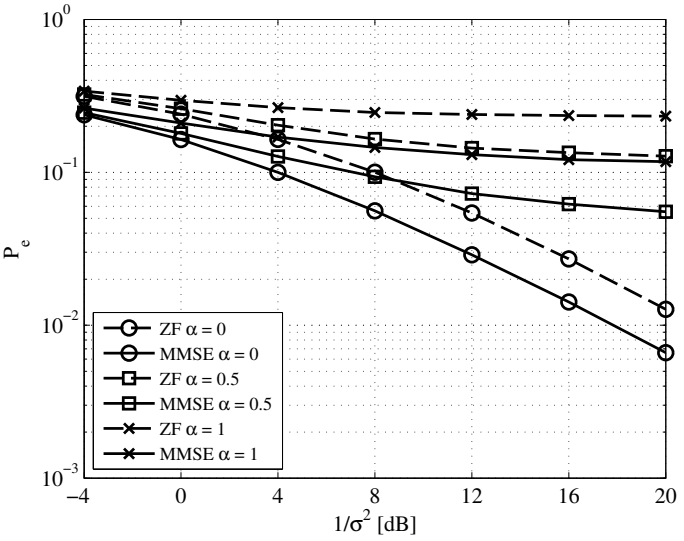

Fig. 6. Comparative probability of bit error (P_e) for the MMSE and ZF equalizer for the secondary (VFDM) system with varying interference levels $\alpha = \{0, 0.5, 1\}$ ($N = 64$, $L = 16$).

equalizers with a constant gap of about 4 dB with respect to to the ZF equalizer. Even though there is no interference coming from the primary system, the MMSE takes into consideration the characteristics of the noise, which explains its best performance among the three. The MF presents the worst performance, with its BER saturating at around 8 dB. The afore mentioned behavior can also be easily seen in terms of throughput in Figure 5. Again we find that the MMSE outperforms the other two equalizers providing a throughput gain of about 500 Kbps at the low SNR regime with respect to the ZF. The MF's throughput is the worst, saturating at about 7 Mbps at the high SNR regime while the other two saturate above the 8 Mbps mark. We must state that, even though MMSE provides the best overall performance, it is still known to be the most complex equalizer of the three analyzed, followed by the ZF and the MF, respectively.

C. VFDM and Interference

In a realistic environment, it will be rare to have a completely faded interference channel ($\alpha = 0$) and thus it is interesting to study the behavior of VFDM in the presence of interference from the primary system. In Figure 6, the P_e curves[1] for the MMSE and ZF equalizers[1] under increasing interference is presented ($\alpha = \{0, 0.5, 1\}$) are presented. As expected, the presence of interference severely degrades the performance of the both equalizers, with higher saturation points for higher interference. In order to better see the effect of the increasing interference levels, we isolated the MMSE equalizer, this time with a bigger interference range ($\alpha = \{0, 0.01, 0.1, 0.5, 1\}$). The P_e curves for such a case can be seen in Figure 6 where the P_e becomes more rapidly sensible to the interference as α approaches 1 (the difference can be barely seen for $\alpha = 0.01$ with respect to $\alpha = 0$ since the separation will occur at higher SNRs). Once more, this

[1]BER curves and MF results are omitted for readability purposes.

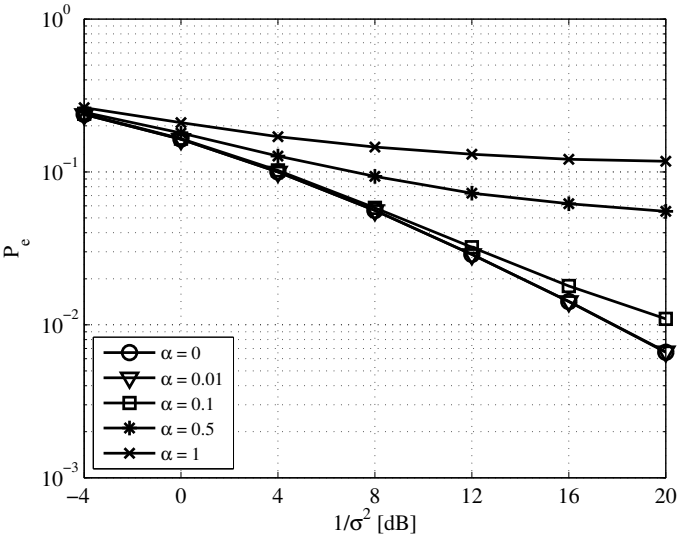

Fig. 7. Comparative probability of bit error (P_e) for the MMSE equalizer for the secondary (VFDM) system with varying interference levels $\alpha = \{0, 0.01, 0.1, 0.5, 1\}$ ($N = 64$, $L = 16$).

behavior is confirmed by the throughput curves, as seen in Figure 8.

V. Conclusions

In this work we have continued the development of a new cognitive radio technology for spectrum re-use and network overlay called VFDM. Unlike in a previous work, we have relaxed the main idealistic assumptions i.e. the use of the ML equalizer and Gaussian codebook. In the current contribution, we have rather studied VFDM's performance using practical linear equalizers, namely the MMSE, ZF and MF using QPSK symbols. Being more specific, we have performed a numerical analysis of the VFDM BER, probability of bit error and sum rate capacity performance with respect to the primary OFDM

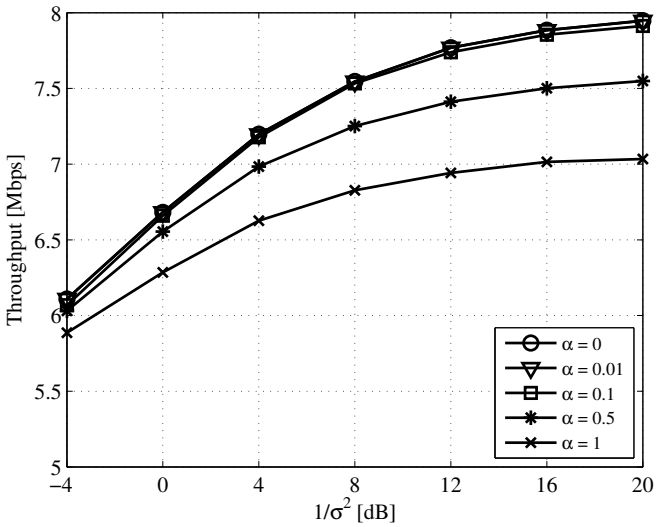

Fig. 8. Comparative throughput T for the MMSE equalizer for the secondary (VFDM) system with varying interference levels $\alpha = \{0, 0.01, 0.1, 0.5, 1\}$ ($N = 64$, $L = 16$).

system and to increasing interference levels. Our main findings are:

- VFDM, also being an orthogonal modulation, performs similar to OFDM in terms of BER;
- VFDM provides a diversity gain at low SNR regime due to the transmit diversity intrinsic to its operation. This happens in spite of the upper bound of N/L on the rate, meaning only that symbols experiencing a low SNR will be more robust, compared to that of OFDM;
- as expected, the MMSE equalizer provides a better performance, with about 4 dB of constant gain over ZF;
- the MF provides the worst performance of the batch saturating its BER and sum rate capacity ($\sim$ 0.4 bps/Hz) at about 12 dB of SNR;
- interference from the primary system severely affects the BER and sum rate capacity performance of the equalizers, with higher sensibility as α approaches 1.

As it was shown in this work, VFDM offers a good performance provided that it exploits the left-over degrees of freedom from the primary system at only the cost of CSI acquisition. In the continuation of this work, we will study the impact of imperfect channel state information on the performance of the secondary system as well as the ability to cancel the interference to the primary system. Furthermore, we will look into the useful data-to-estimation symbols proportion in order to provide a good performance tradeoff. Then, we will propose the implementation of a feasible multi-user system based on VFDM. Finally we will continue the implementation of VFDM on a transmission testbed as a proof of concept.

REFERENCES

[1] S. E. W. Group, "Report of the spectrum efficiency working group," FCC, Tech. Rep., November 2002.

[2] J. Mitola, "Cognitive radio an integrated agent architecture for software defined radio," Ph.D. dissertation, Royal Institute of Technology (KTH), May 2000.

[3] J. Peha, "Approaches to spectrum sharing," *Communications Magazine, IEEE*, vol. 43, no. 2, pp. 10–12, 2005.

[4] L. S. Cardoso, M. Debbah, S. Lasaulce, M. Kobayashi, and J. Palicot, *Cognitive Radio Networks: Architectures, protocols and standards*. Taylor&Francis Group, 2008, ch. Spectrum Sensing in Cognitive Radio Networks, unpublished.

[5] S. Haykin, "Cognitive radio: Brain-empowered wireless communications," *Selected Areas in Communications, IEEE Journal on*, vol. 23, no. 2, pp. 201–220, 2005.

[6] A. Ghasemi and E. S. Sousa, "Fundamental limits of spectrum-sharing in fading environments," *Wireless Communications, IEEE Transactions on*, vol. 6, no. 2, pp. 649–658, 2007.

[7] N. Devroye, P. Mitran, and V. Tarokh, "Achievable rates in cognitive radio channels," *IEEE Transactions on Information Theory*, vol. 52, no. 5, pp. 1813–1827, 2006.

[8] V. Cadambe and S. Jafar, "Interference alignment and degrees of freedom of the k-user interference channel," *IEEE Transactions on Information Theory*, vol. 54, no. 8, pp. 3425–3441, 2008.

[9] S. Perlaza, N. Fawaz, S. Lasaulce, and M. Debbah, "From Spectrum Pooling to Space Pooling: Opportunistic Interference Alignment in MIMO Cognitive Networks," *Arxiv preprint arXiv:0907.1255*, 2009.

[10] L. Cardoso, M. Kobayashi, Ø. Ryan, and M. Debbah, "Vandermonde frequency division multiplexing for cognitive radio," in *Proceedings of the 9th IEEE Workshop on Signal Processing Advances in Wireless Communications (SPAWC'08)*, 2008, pp. 421–425.

[11] G. Golub and C. Van Loan, *Matrix Computations*. Johns Hopkins University Press, 1996.

[12] L. S. Cardoso, M. Kobayashi, and M. Debbah, "Vandermonde-subspace frequency division multiplexing," *Under preparation*, 2010.

[13] M. Kobayashi, M. Debbah, and S. Shamai, "Secured communication over frequency-selective fading channels: A practical Vandermonde precoding," 2009.

[14] D. Tse and P. Viswanath, *Fundamentals of Wireless Communication*. Cambridge University Press, 2005.

[15] L. Rabiner and B. Gold, *Theory and application of digital signal processing*. Prentice-Hall, 1975.

[16] S. Verdu, *Multiuser Detection*. Cambridge University Press, 1998.

[17] J. Proakis and M. Salehi, *Digital Communications*. McGraw-hill New York, 1995.

[18] "Ansi/ieee standard 802.11," ANSI/IEEE, Tech. Rep., 1999.